Non-uniform central airways ventilation model based on vascular segmentation

G. Ibrahim
Department of Engineering, University of Leicester
University Road, Leicester, LE1 7RH, UK
gi12@leicester.ac.uk

A. Rona[1]
Department of Engineering, University of Leicester
University Road, Leicester, LE1 7RH, UK
ar45@leicester.ac.uk

S. V. Hainsworth
Department of Engineering, University of Leicester
University Road, Leicester, LE1 7RH, UK
svh2@leicester.ac.uk

[1] Corresponding author, Tel: +44 116 252 2510, Fax: +44 116 252 2619.

Abstract

Improvements in the understanding of the physiology of the central airways require an appropriate representation of the non-uniform ventilation at its terminal branches. This paper proposes a new technique for estimating the non-uniform ventilation at the terminal branches by modelling the volume change of their distal peripheral airways, based on vascular segmentation. The vascular tree is used for sectioning the dynamic CT-based 3D volume of the lung at 11 time points over the breathing cycle of a research animal. Based on the mechanical coupling between the vascular tree and the remaining lung tissues, the volume change of each individual lung segment over the breathing cycle was used to estimate the non-uniform ventilation of its associated terminal branch. The 3D lung sectioning technique was validated on an airway cast model of the same animal pruned to represent the truncated dynamic CT based airway geometry. The results showed that the 3D lung sectioning technique was able to estimate the volume of the missing peripheral airways within a tolerance of 2%. In addition, the time-varying non-uniform ventilation distribution predicted by the proposed sectioning technique was validated against CT measurements of lobar ventilation and showed good agreement. This significant modelling advance can be used to estimate subject-specific non-uniform boundary conditions to obtain subject-specific numerical models of the central airway flow.

Keywords: Non-uniform ventilation; Bronchial flow modelling; Physiological boundary conditions; CT image processing; Vascular segmentation.

1 Introduction

Airflow analysis underpins the understanding of lung physiology and pulmonary target therapy. However, performing this analysis, either clinically or by in vivo experiments, is challenging due to the inaccessible nature of the lungs. For this reason, current research efforts are focusing on the numerical modelling of the central airways using subject-specific geometries extracted from volumetric medical imaging data, such as four-dimensional computed tomography (4DCT). A reliable numerical modelling of the central airway flow requires the appropriate representation of the tracheal bulk flow and of the non-uniform ventilation at its terminal branches imposed by the peripheral airways that are not captured by 4DCT.

Few attempts have been made to approximate the effect of the non-uniform ventilation at the terminal branches when numerically modelling the bronchial flow. De Backer et al. [1] iteratively imposed different pressure values at the terminal branches of the left and the right lungs so that the numerically predicted mass flow towards the left and right lung reflected the proportional lung growth measured from CT images acquired at two different inflation levels. De Backer et al. [2] and Lambert et al [3] adopted a similar iterative approach based on CT measurements of lobar growth rather than of lung growth. Although such iterative approaches improved the reliability of the numerical predictions of the central airway flow, they are not adequate to accurately capture the non-uniform inner lobar flow distribution. Yin et al. [4, 5] used a 3D-1D coupling model associated with a ventilation map computed by registering CT images acquired at different inflation levels to estimate the flow at the

terminal branches based on mass conservation. Their technique resulted in a good approximation to the CT measurement of lobar ventilation. However, the 1D model in their study uses lobe-averaged volumetric airflow data. The apportionment of the lobar ventilation among its terminal branches has to be assumed, which may increase the uncertainty of the predicted ventilation within each lobe.

Together with the bronchial airways, the pleural cavity encloses the vascular tree, which is responsible for conducting the blood between the heart and the alveolar sacs where gas exchange takes place. The pulmonary arteries run alongside the bronchial airways and the pulmonary veins show a similar branching pattern to the arteries, though separated from them [6]. The topology of the pulmonary veins divides the lung lobes into several segments known as the bronchopulmonary segments. These segments are separated from each other by connective tissue septa that cannot be identified in low-resolution CT images [7]. Each segment is supplied by a segmental bronchus and its accompanying pulmonary artery branch [8]. This pulmonary artery and its peripheral arteries are tethered to the surface of their adjacent airways and to the lung parenchyma via a connecting tissue [9]. In the conducting zone of the lung, the pulmonary arteries that accompany the conducting airways tend to retain their shape during breathing as they contain a number of smooth muscles and a large volume of blood passing through them. However, they stretch and displace in accordance to their adjacent airways during breathing as a result of that tethering [10-12]. In the respiratory zone of the lung, where most of the lung volume change takes place during breathing, more of the adventitial surface of the arteries (and veins) is tethered to the surrounding lung parenchyma [9] and the smooth muscles surrounding

the blood vessels are less present. Hence, the overall structure (position, diameter and length) of the arteries (and veins) in the respiratory zone varies in accordance to the change in the lung volume during breathing [13-16]. This indicates a mechanical coupling between the lung tissues and the pulmonary arteries and veins in the pleural cavity. By this mechanical coupling, the deformation of the vascular tree in accordance to the change in lung volume during breathing can be used to approximate the volume change of the missing peripheral airways distal to each terminal branch.

In this paper, a sectioning technique is proposed to segment a time sequence of 3D volumes of the sampled breathing cycle of a laboratory animal into several segments, where each segment encloses the volume of the missing peripheral airways distal to each terminal branch. The corresponding segments are defined based on the mechanical coupling between the vascular tree and the lung tissues. The computed volume change of the individual segments is then used to estimate the non-uniform ventilation at the terminal branches of the central airways. The proposed sectioning technique is validated on a cast geometry of the bronchial airways of the same animal coupled to a CT based reconstructed vascular tree. In addition, the accuracy of the proposed technique in approximating the volume change of specific segments within the lung during breathing is validated by CT measurements of lobar regional ventilation. Finally, the application of the proposed technique is considered for estimating subject-specific physiological flow boundary conditions to bridge the gap between the numerical modelling of the central airway flow and the actual flow within a living lung.

2 Methodology

2.1 Non-uniform ventilation model overview

The block diagram shown in Figure 1 illustrates the overall process of defining the non-uniform ventilation model. The proposed technique was implemented using multiple dynamic CT images that sampled the breathing cycle of a laboratory animal, as shown in Figure 1 (a). The dynamic CT images were initially processed to generate lung volume masks that cover the lung sac containing the extra-alveolar blood vessels (the pulmonary arteries and the pulmonary veins) as shown in Figure 1 (b). These lung volume-masks were then used to generate 3D geometries of the lung volumes as shown in Figure 1 (c). In addition, 3D geometries of the vascular tree were reconstructed out of the lung volume masks. The generated vascular tree geometries were then synchronised to their corresponding 3D lung volume geometries. Next, the veins that define the bronchopulmonary segments of the lung and the arteries running alongside the missing peripheral airways distal to each terminal branch were identified and extracted out of the vascular tree geometries. The skeleton of the extracted veins were first used to generate sectioning surfaces that define the bronchopulmonary segments of the lung. Then, midline curve segments were generated between the opposing peripheral artery pairs distal to each two adjacent terminal branches using their skeleton. A sectioning surface is then extracted from each midline curve and projected onto the surfaces boundaries of its enclosing bronchopulmonary segment using short distance projection.

As a result, each bronchopulmonary segment of the lung is sectioned into smaller segments where each specific lung segment encloses the missing airways distal to a specific terminal branch as shown in Figure 1 (d). Finally, the volume change of these segments was used to estimate the non-uniform ventilation for their associated terminal branch.

2.2 Dynamic CT imaging and airway geometry sampling

11 CT images were acquired dynamically for a 298g male Sprauge-Dawley rat at the Pacific Northwest national laboratory, Washington, USA. The animal use was approved by their affiliated institutional animal care and use committee (Protocol 2010-23). The imaging process is extensively explained in [17]. Briefly, the rat was anesthetised and then intubated with a 4 cm long 14-gauge catheter tube and connected to the commercial ventilator from CWE Inc. (Model 830/AP, Ardmore, PA). The ventilator was set to deliver air (30% O_2, 70% N_2) at 54 tidal breaths per minute (500 ms inspiration, 600 ms expiration, and ~6.2 cmH_2O Peak Inspiratory Pressure (PIP)). The rat was scanned supine using the commercial micro-CT scanner eXplore (Model CT120, GE Health Care Waukesha, WI). Scanning parameters were 80 kVp, 32 mA, 16 ms exposure time, 100 μm resolution, 360° projection with 1° increment. Figure 2 (a) illustrates the CT imaging time points superimposed on a typical flow volume change waveform measured by the ventilator unit.

The medical image processing software Mimics (Materialize, Belgium) was used to segment and reconstruct a 3D geometry of the bronchial airways out of each CT image. The segmentation process was done automatically following the intensity threshold

approach. This segmentation required some additional manual adjustments to ensure the surface boundary continuity of the bronchial tree cross-sections. The generated 3D geometries were limited to 4±1 generations, resulting in 28 terminal branches as shown in Figure 2 (b). The image quality of the dynamic CT data set was not sufficient to reconstruct additional generations. Each airway geometry was manually cleaned up and the axial boundary surfaces were defined perpendicular to the centreline of their associated airway geometry.

2.3 Computation and 3D sampling of the lung volume

A mask covering the lungs and a small zone of the extra-alveolar vessels was generated from each CT image following the steps proposed in [18]. First, a Gaussian 3D filter (radius =1) was applied to the image slices. Then, the 3D Toolkit plugin within the free source software ImageJ (NIH, Bethesda, Maryland, USA) was used to generate the lung volume mask for each CT-image by inserting a seed point within the lung. Finally, the 3D Dilate and the 3D Erode functions, also available within the 3D toolkit of ImageJ, were applied to the generated masks in order to fill the missing voxels and smooth the boundaries. Figure 3 (a) illustrates the calculated mask on a sample slice. 3D geometries were then reconstructed out of the generated masks using the commercial software Mimics. The volume change of the 3D geometries was calculated and compared to the lung volume change measured by the ventilator unit as shown in Figure 3 (b). It can be seen that the change in the volume measured from the sequence of the 3D geometries matches well the lung volume change measured by the ventilator unit. The partitioning of the 3D geometries in lung volume segments shown in Figure

1(d) uses sectioning surfaces of zero thickness, so that the sum of the sectioned volumes is equal to the un-split 3D geometry volume, by construction. This method is volume conservative and enables to assume that the volume change of corresponding segments in the mask-based 3D geometry time sequence reflects the volume change of the same segment within the living lung.

2.4 Segmentation and 3D sampling of the vascular tree

Unlike the bronchial airways, the vascular tree has a distinguishable x-ray opacity comparable to that of bones, which makes it visible almost down to the capillaries in CT scans with high resolution. However, identifying and segmenting the vascular tree in dynamic CT data is more challenging due to the low resolution of the acquired images. Hence, it was necessary to enhance the contrast of the vascular tree for an easier segmentation. To do this, the lung was extracted from the CT images by applying the lung volume-masks generated in section 2.3 to the original CT images using the image calculator tool in ImageJ. An enhance contrast function with histogram equalization was then applied to the digitally masked lung cross-section images in order to improve the contrast between the vascular tree and the other lung tissues. Finally, a tubeness filter [19], available within ImageJ, was applied to the contrast enhanced images. This filter examines the connectivity between the pixels within the data set based on the eigenvalues of the Hessian matrix. A sample of the resulting images is shown in Figure 4 (a). 3D geometries of the vascular tree were then reconstructed by assembling the tubeness-filtered cross-sections. Some manual processing of the 3D surfaces was required to repair open vessel walls and to properly

connect smaller vessels to their parent vessels. A sample geometry of the reconstructed vascular tree superimposed on its associated 3D airway geometry is shown in Figure 4 (b). It can be seen that the generated 3D geometry of the vascular tree adventitial surface is coarse. This is mainly due to the low spatial resolution of the dynamic CT data set (0.1 mm). However, as only the centreline of the blood vessels will be used to segment the 3D volumes of the lung, the roughness of the adventitial surface is not a concern for the implementation of the lung volume sectioning algorithm detailed in section 2.5.

2.5 Sectioning the lung volume geometry

Figure 5 (a) illustrates the airway segments generated for a sample airway volume. The steps followed to generate these segments are illustrated on a sample terminal branch shown in Figure 5 (b.1). To define the boundaries of the desired lung volume segments, the veins that outline the bronchopulmonary segments of the lung and the arteries running alongside the outer branches of the missing airways distal to each terminal branch were extracted from the vascular tree geometries as shown in Figure 5 (b.2). The extracted veins and arteries are referred to as the blood vessels of interest. Following the extraction process, centreline segments were automatically generated for the blood vessels of interest using the 3D thinning algorithm of Palágyi et al. [20]. Let C_v designate the centreline segments of the extracted veins and C_a designate the centreline segments of the extracted arteries as shown in Figure 5 (b.4). Due to the low resolution of the dynamic CT data set, some of the small veins and arteries at the tips of the vascular tree geometries were missing. Therefore, the connection between the

vessels of interest and the visceral pleura was missing and had to be approximated. This was done by projecting the end-points of each C_v and C_a on the wall of the visceral pleura. These points were then used to bridge the gaps between the centreline segments and the visceral pleura using straight lines. Additionally, since the structure of the arteries within the vascular tree follow the same branching pattern of the missing airways, midline curve segments C_m were generated between the opposing artery pairs associated to each terminal branch based on the structure of their centreline segments C_a as shown in Figure 5 (b.4). The midline tool, available in the commercial software ICEM CFD (ANSYS, USA), was used to generate these centrelines. The generation of C_m was a semi-automated process as it required the user to designate opposing artery centreline pairs from which each C_m was generated.

Sectioning the 3D lung volume geometries was performed following two main steps. First, the bronchopulmonary segments of the lungs were identified by generating sectioning surfaces that define the boundaries of each bronchopulmonary segment using the centreline segments of the extracted veins C_v as shown in figure 5 (b.5). Then, the defined bronchopulmonary segments were further sectioned into smaller segments where necessary using the arteries midline curve segments C_m. This was done by generating a sectioning surface between each C_m and its short distance projection onto the boundary surfaces of the bronchopulmonary segment enclosing C_m, so that each lung volume segment enclosed only one terminal branch as shown in figure 5 (b.6). Note that lobar boundaries were not used for generating the lung volume segments. This was done deliberately to enable the use of this geometrical data for the a-posteriori validation of the sectioning technique reported in section 3.2.

Since the vascular tree is tethered to the bronchial airways and to the lung parenchyma, it was assumed that the shape and the position of the generated segmental boundaries vary in accordance to the change in the lung volume during breathing. Thus, the volume change of the individual segments reflects the volume change of their enclosed airways. Hence, the volume change of the individual segment can be used to estimate the non-uniform ventilation for their associated terminal branches using the following equation

$$Q = \frac{d(V_S - V_G)}{dt} \quad (1)$$

where Q is the volumetric flow rate, V_S is the volume of the lung segment associated to a given terminal branch, V_G is the volume of the CT based airway geometry enclosed within the same lung segment, and t is the breathing time.

3 Results

3.1 Evaluation of the sectioning technique on an airway cast

To evaluate the accuracy of the proposed technique in defining the lung volume associated to each terminal surface, the proposed sectioning process was applied to a cast geometry of the bronchial airways extracted from the same animal post-mortem. The cast geometry was coupled to a vascular tree geometry of the animal reconstructed out of a CT image acquired at approximately the same inflation level as the cast geometry. Airway casting and animal imaging were performed by a research group at the at the Pacific Northwest national laboratory, Washington, USA. The

animal imaging process and airway casting are extensively explained in Jacob et al. [21]. Briefly, the rat was subjected to euthanasia using CO_2 asphyxiation, and then intubated with a 14-gage catheter tube. A ventilator unit was then used to inflate the rat lungs to its Total Lung Capacity (TLC) at ~25 cmH_2O. At that time, the lungs were scanned using the commercial micro-CT scanner (eXplore CT120, GE Health Care Waukesha, WI). Scanning parameters were 90 kVp, 40 mA, 16 ms exposure time, 50 µm resolution, 360° gantry rotation with 900 projections. Following the scanning process, an in-situ rigid cast of the rat bronchial tree was made following the methodology of Phalen et al. [22]. The lungs were degassed and held inflated at ~30 cmH_2O. A pre-calculated lung volume of ~2.3 mL of a casting agent was then slowly injected into the lungs in-situ via the intubated catheter tube. The casting agent mix consisted of 10 g Dow-Corning 734 flowable sealant, 3.7 g Dow-Corning 200 fluid, and 1.3 g of Ultravist (iopromide, Bayer HealthCare), and an iodine-based CT contrast agent [21]. Finally, a CT image of the rat thorax was acquired using the same scanning parameters used for imaging the lung at TLC.

A 3D geometry of the airway cast was then automatically segmented and reconstructed out of the cast images. The segmentation process did not require any pre-processing steps. This is due to the CT contrast agent that was added to the cast materials which makes it distinguishable in the CT image. The reconstructed cast geometry included a high number of airway generations that are significantly beyond the resolution of the 4DCT images of living animals. Each additional generation is morphologically connected to a specific terminal branch of the CT images and, therefore, should be contained in the lung volume section associated to this specific

branch. The vascular tree of the animal was segmented and reconstructed out of the TLC image acquired prior to the casting process following the same steps discussed in section 2.4. A 3D geometry of the bronchial airways was also segmented and reconstructed out of the TLC image following the steps discussed in section 2.2. The airway cast geometry was aligned to this CT based airway geometry in order to attach the airway cast geometry to the geometry of the CT based vascular tree as shown in Figure 6. It can be seen from the magnification window in Figure 6 that the blood arteries run alongside the bronchial tree and follow a similar branching pattern.

The airway cast geometry was pruned to represent the geometry of the bronchial airways with a reduced number of generations similar to that obtained from the dynamic CT scans (4±1 generations with 28 terminal branches). The sectioning technique was then applied to the pruned cast geometry in order to estimate the sections of the lung volume associated to each terminal branch. The actual section of the lung associated to each terminal branch was determined by referring back to the unpruned airway cast geometry. Figure 7 illustrates the sectioning process applied to the right cranial lobe of the animal lungs. It can be seen that the proposed sectioning technique was able to successfully define segments within the lung volume that wrap and separate the missing peripheral airways of the terminal branches. However, minor geometrical violations were observed on some of the generated segments of the animal lungs similar to the one shown in the magnification window in Figure 7 (d). Figure 7 (d) shows some of the airway branch tips from the cast airway geometry dipping into the neighbouring volume section. The volume of the misinterpreted airway geometries within the lung volume segments was less than 2% compared to the

volume of the enclosed airway branches. Such a small error is not expected to significantly affect the accuracy of the estimated non-uniform ventilation.

3.2 Validation of the non-uniform bronchial ventilation model

Section 3.1 provided a validation test for the non-uniform sectioning of the lung volume among the terminal branches at TLC. This section addresses the validation of the non-uniform ventilation model by evaluating the non-uniform ventilation distribution among the five lobes over the tidal breathing cycle of the laboratory animal. Figure 8 illustrates the comparison between the lobar volumes at different time points computed following the proposed sectioning technique to that measured from the CT scans. The CT measurement of the lobar volume was done by segmenting the lobes from the CT images following the fissure lines. The purpose of this comparison was to validate the accuracy of approximating the time dependant volume of a specific lobe within the lung using the proposed technique.

No significant discrepancy was observed between the computed and the measured volume at all the investigated time points over the breathing cycle. The proposed technique was able to accurately predict the lobar volume at different times with a maximum error of less than 2.5%. Since this section does not provide a validation of the non-uniform bronchial ventilation for the individual terminal surfaces, it is important to note that the lobes are the smallest morphologically defined segments of the lung in a CT scan since the fissure lines separate them. Therefore, validating

against the change in the lobes volume is a good indication of the accuracy of the proposed technique.

4 Discussion and limitations

The proposed non-uniform ventilation model provides the ability to define dynamic physiological boundary conditions for the numerical modelling of the central airway flows depending mainly on biometrical information extracted from the lungs using dynamic CT scans. This technique has significant and substantial differences with respect to algorithms used in previous work, which either relied on the volume change of the overall lungs or that of individual lobes [1, 2, 4, 5] to approximate the boundary conditions for flow modelling applications. The boundary conditions that can be defined by the proposed technique use additional physiological information in the form of the vascular tree that was not used in past work. This greater use of subject-specific data is conducive to obtaining more reliable numerical predictions of the bronchial flow compared to that of a living lung. However, important limitations and uncertainties remain to be addressed. Firstly, the proposed sectioning technique of the lung volume depends on the mechanical coupling between the vascular tree and the lung tissues. This mechanical coupling, whilst present throughout the bronchial tree, exhibits zonal variations. Although the arteries are accompanying the bronchial airways down to the alveolar sacs, the amount of their adventitial surface that is tethered to their adjacent airways vary widely from dorsal to apex [9]. Similarly, the tethering between the veins and the lung tissues is complex and inhomogeneous. Moreover, the volume of the smooth muscles surrounding the arteries and the veins

vary widely from dorsal to apex and the volume of the blood flowing through each vessel varies. All these elements may affect the elasticity and, hence, the deformation pattern of the blood vessels during breathing with respect to the deformation in the lung volume. Since many of these effects have not been systematically investigated, the assumption that the vascular tree deforms in accordance to the change in the lung volume during the breathing cycle should be investigated further. In addition, there are significant morphological differences between the vascular trees of rats and humans. The human vasculature is relatively thicker and has a larger volume compared to the rat vasculature. Therefore, it should be possible to render the human vascular tree as readily as in rats using a similar filtration approach [23]. However, the presence and the number of the elastic laminae and the degree of the muscularity vary widely in the vasculature of humans and rats [24]. Thus, as the validation of the proposed technique was limited to a rat model, its direct application on humans requires further analysis.

Another limitation affecting the accuracy of the proposed sectioning technique and, hence, the reliability of the derived dynamic subject-specific boundary conditions is the ability of identifying and segmenting the lower vessels of the vascular tree (the arterioles, the venules, and the capillaries) out of the CT images. This limitation manifests particularly when dealing with a low-resolution CT data set similar to that of the dynamic CT imaging used in this study. The missing blood vessels are likely to affect the accuracy of the lung volume sectioning since the coupling between the segmented vascular tree and the inner pleural membrane (the visceral pleura) has to be

approximated. This may result in imprecise but still acceptable dynamic physiological boundary conditions.

Conclusions

This paper introduces a lung volume sectioning technique based on vascular segmentation to estimate the non-uniform ventilation within the peripheral airways that are not captured by currently available 4DCT imaging techniques. The motivation for modelling the subject-specific non-uniform ventilation is the prospective of using subject-specific numerical models for investigating the flow within patient-specific geometries of the central airways.

The vascular tree was used as a reference to section the lung volume generated from successive 4DCT images that sample the breathing cycle into several segments, where each segment encloses the missing peripheral airways associated to each CT captured terminal airway branch. Since the vascular tree is mechanically coupled to the bronchial tree and the lung parenchyma, the volume change of the corresponding segments defined by the vascular tree over the breathing cycle is expected to reflect the volume change of the same segment within a living lung. Therefore, the volume change of the corresponding lung segments defined by the vascular tree was used to estimate the non-uniform ventilation for their enclosed terminal branches.

Using a cast model, the proposed sectioning technique was found to be able to successfully estimate the volume of the missing peripheral airways at TLC within a tolerance of 2%. Furthermore, the ability of the proposed technique in approximating

the volume change of specific segments of the lungs over time during breathing was validated by comparing CT measurements of the lobar volume change to that computed following the proposed technique. Although the maximum observed discrepancy between the measured and the computed lobar volume change was less than 2.5%, this strategy is not sufficient to fully validate the capability of the proposed technique in estimating the non-uniform ventilation of the missing peripheral airways distal to each individual terminal branch.

The significant output from this research is the availability of a technique that can be used to develop dynamic physiological boundary conditions for the numerical modelling of the central airway flow depending mainly on biological information obtained from the lung deforming constituents. This is different to the previously published algorithms that use the global lung (or lobes) volume change or empirical flow volume fraction models of the bronchial airways to predict non-uniform ventilation effects.

Acknowledgment

The authors would like to thank Richard Jacob of the Biological Sciences Division in the Pacific Northwest National Laboratory, Washington, USA for supplying the animal data used in this study.

References

[1] J.W. De Backer, W.G. Vos, C.D. Gorlé, P. Germonpré, B. Partoens, F.L.Wuyts, P.M. Parizel, Flow analyses in the lower airways: Patient-specific model and boundary conditions, Medical Engineering & Physics, 30 (2008) 872-879.

[2] J.W. De Backer, W.G. Vos, S.C. Vinchurkar, R. Claes, A. Drollmann, D. Wulfrank, P.M. Parizel, P. Germonpré, W.D. Backer, Validation of computational fluid dynamics in CT-based airway models with SPECT/CT, Radiology:, 257 (2010) 854-862.

[3] A.R. Lambert, P. O'Shaughnessy, M.H. Tawhai, E.A. Hoffman, C.L. Lin, Regional deposition of particles in an image-based airway model: large-eddy simulation and left-right lung ventilation asymmetry, Aerosol Sci Technol, 45 (2011) 11-25.

[4] Y. Yin, J. Choi, E.A. Hoffman, M.H. Tawhai, C.L. Lin, Simulation of pulmonary air flow with a subject-specific boundary condition, Journal of Biomechanics, 43 (2010) 2159–2163

[5] Y. Yin, J. Choi, E.A. Hoffman, M.H. Tawhai, C.-L. Lin, A multiscale MDCT image-based breathing lung model with time-varying regional ventilation, Journal of Computational Physics, (2013) 168-192.

[6] A.A. Hislop, Airway and blood vessel interaction during lung development, Journal of anatomy, 201 (2002) 325-334.

[7] R. O'Rahilly, R. Swenson, F. Muller, S. Carpenter, B. Catlin, Basic human anatomy, Philadelphia: WB Saunders, 162 (1983).

[8] R. Drake, A.W. Vogl, A.W.M. Mitchell, Gray's anatomy for students, Philadelphia, PA : Churchill Livingstone/Elsevier2010.

[9] M.I. Townsley, Structure and Composition of Pulmonary Arteries, Capillaries, and Veins, Comprehensive Physiology, John Wiley & Sons, Inc.2011.

[10] J.J. Benjamin, P.S. Murtagh, D.F. Proctor, H.A. Menkes, S. Permutt, Pulmonary vascular interdependence in excised dog lobes, J Appl Physiol, 37 (1974) 887-894.

[11] J. Kalk, J. Benjamin, H. Comite, G. Hutchins, R. Traystman, H. Menkes, Vascular interdependence in postmortem human lungs, The American review of respiratory disease, 112 (1975) 505-511.

[12] S.J. Lai-Fook, A continuum mechanics analysis of pulmonary vascular interdependence in isolated dog lobes, Journal of applied physiology: respiratory, environmental and exercise physiology, 46 (1979) 419-429.

[13] B.H. Culver, J. Butler, Mechanical Influences on the Pulmonary Microcirculation, Annual Review of Physiology, 42 (1980) 187-198.

[14] A.L. Mansell, A.L. McAteer, A.C. Pipkin, Maturation of interdependence between extra-alveolar arteries and lung parenchyma in piglets, Circ Res, 71 (1992) 701-710.

[15] R.K. Albert, W.J. Lamm, D.A. Rickaby, A. Al-Tinawi, C.A. Dawson, Lung inflation distends small arteries (< 1 mm) in excised dog lungs, J Appl Physiol (1985), 75 (1993) 2595-2601.

[16] R.A. Rhoades, Respiratory physiology, in: R.A. Rhoades, D.R. Bell (Eds.) Medical physiology: principles for clinical medicine, Lippincott Williams & Wilkins, Philadelphia, 2009.

[17] R. Jacob, W. Lamm, Stable small animal ventilation for dynamic lung imaging to support computational fluid dynamics models, PLoS ONE, 6 (2011).

[18] R.E. Jacob, J.P. Carson, M. Thomas, D.R. Einstein, Dynamic Multiscale Boundary Conditions for 4D CT of Healthy and Emphysematous Rats, PLoS ONE, 8 (2013) e65874.

[19] Y. Sato, S. Nakajima, N. Shiraga, H. Atsumi, S. Yoshida, T. Koller, G. Gerig, R. Kikinis, Three-dimensional multi-scale line filter for segmentation and visualization of curvilinear structures in medical images, Med Image Anal, 2 (1998) 143-168.

[20] K. Palágyi, E. Sorantin, E. Balogh, A. Kuba, C. Halmai, B. Erdohelyi, K. Hausegger, A sequential 3D thinning algorithm and Its medical applications, in: M.F. Insana, R.M. Leahy (Eds.) IPMI 'Proceedings of the 17th International Conference on Information Processing in Medical Imaging Springer-Verlag, Berlin Heidelberg, 2001, pp. 409-415.

[21] R.E. Jacob, S.M. Colby, S. Kabilan, D.R. Einstein, J.P. Carson, In situ casting and imaging of the rat airway tree for accurate 3D reconstruction, Experimental Lung Research, 39 (2013) 249-257.

[22] R.F. Phalen, H.C. Yeh, O.G. Raabe, D.J. Velasquez, Casting the lungs In-situ, Anat Rec, 177 (1973) 255-263.

[23] H. Shikata, G. McLennan, E.A. Hoffman, M. Sonka, Segmentation of pulmonary vascular trees from thoracic 3D CT images, International Journal of Biomedical Imaging, 2009 (2009) 636240.

[24] M.I. Townsley, Structure and composition of pulmonary arteries, capillaries and veins, Comprehensive Physiology, 2 (2012) 675-709.

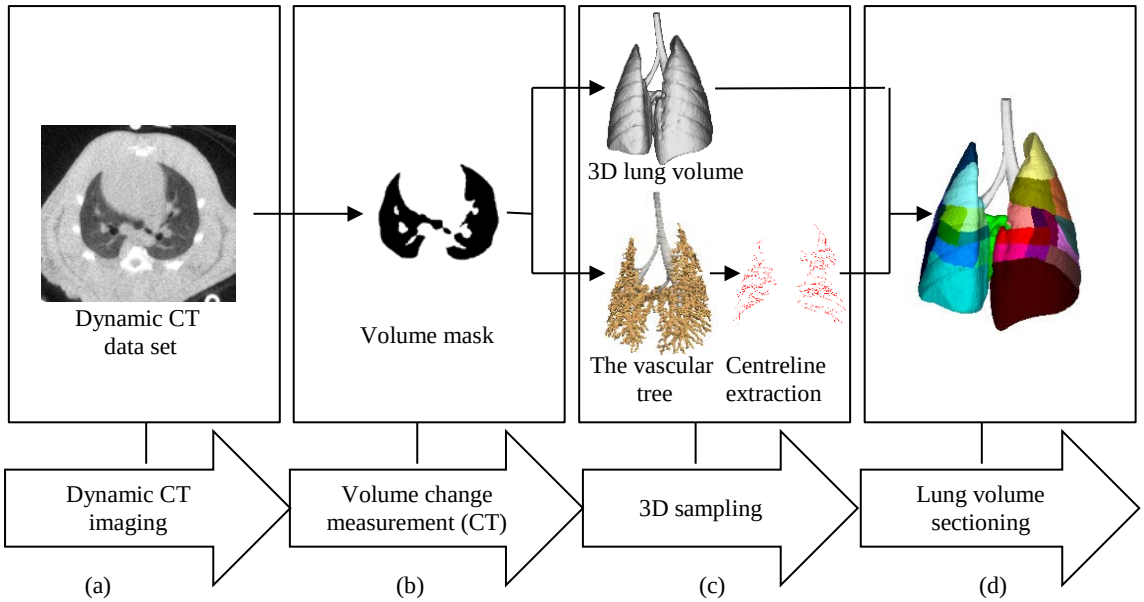

Figure 1: Block diagram of deriving defining the non-uniform ventilation model.

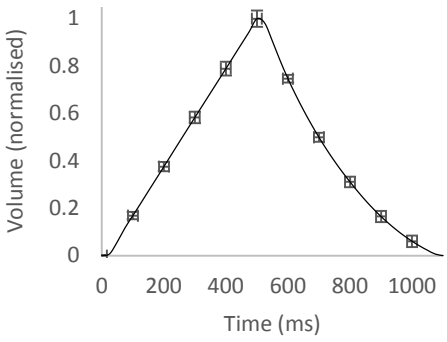

(a)

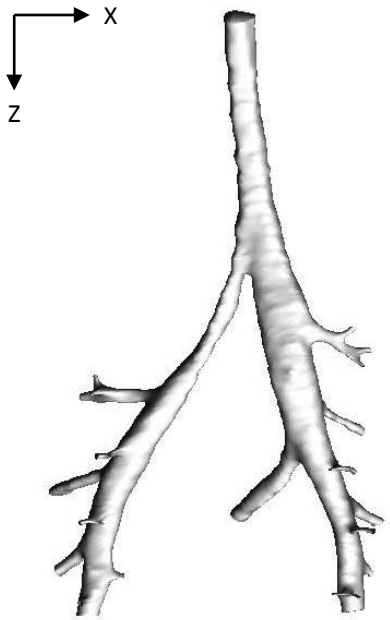

(b)

Figure 2: (a) CT image time points superimposed over a typical breathing cycle imposed by the ventilator. The width of the bars represents the 16 ms exposure time and the height of the bars represents the standard deviation. (b) A sample of the reconstructed airway geomtries at t = 0 ms.

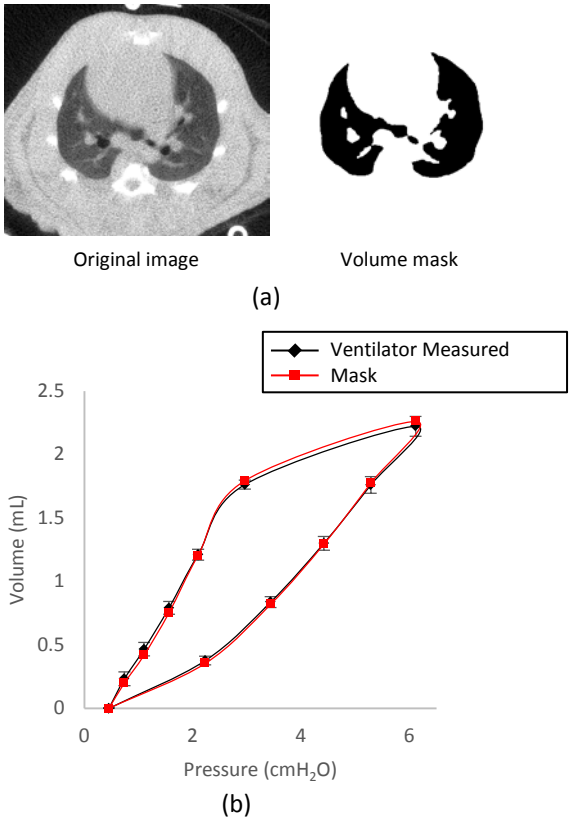

Figure 3: (a) the computed lung volume-mask illustrated on a sample slice, (b) a comparison of the average ventilator-measured lung volume change and the total volume change measured from the lung 3D geometries. The error bars represent the standard deviation of the ventilator measurements.

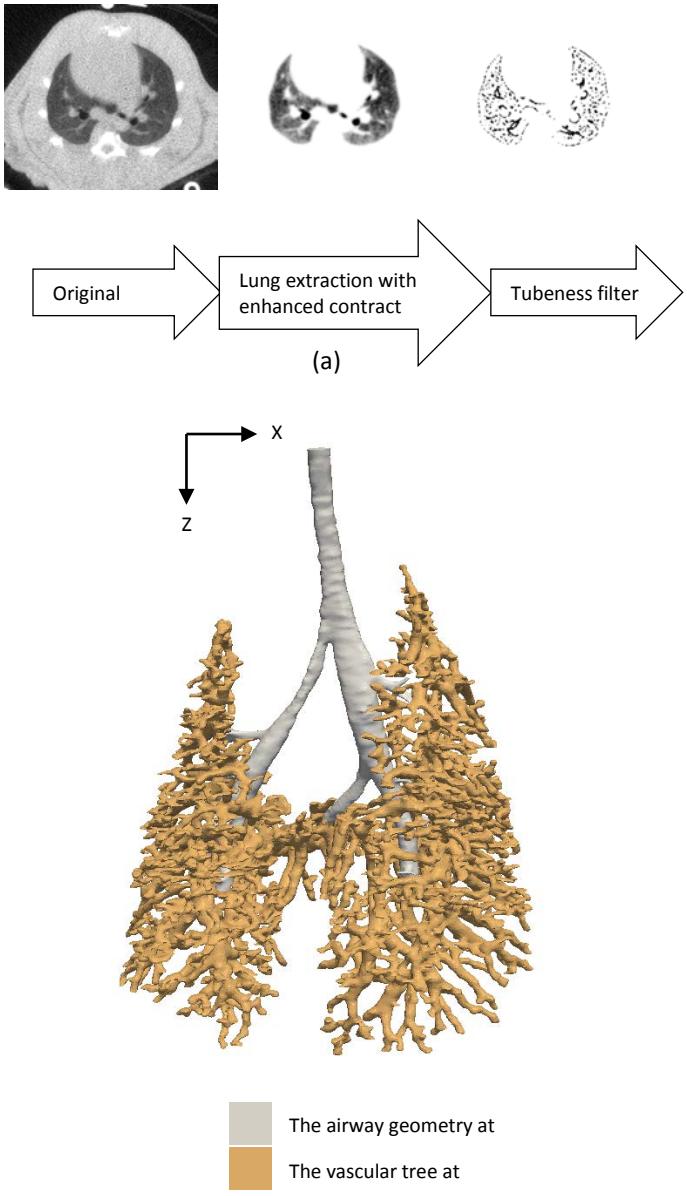

Figure 4: (a) CT image pre-processing for the segmentation and transverse plane sampling of the vascular tree out of the dynamic CT data set. (b) 3D rendering of a sample vascular tree superimposed on its associated airway geometry.

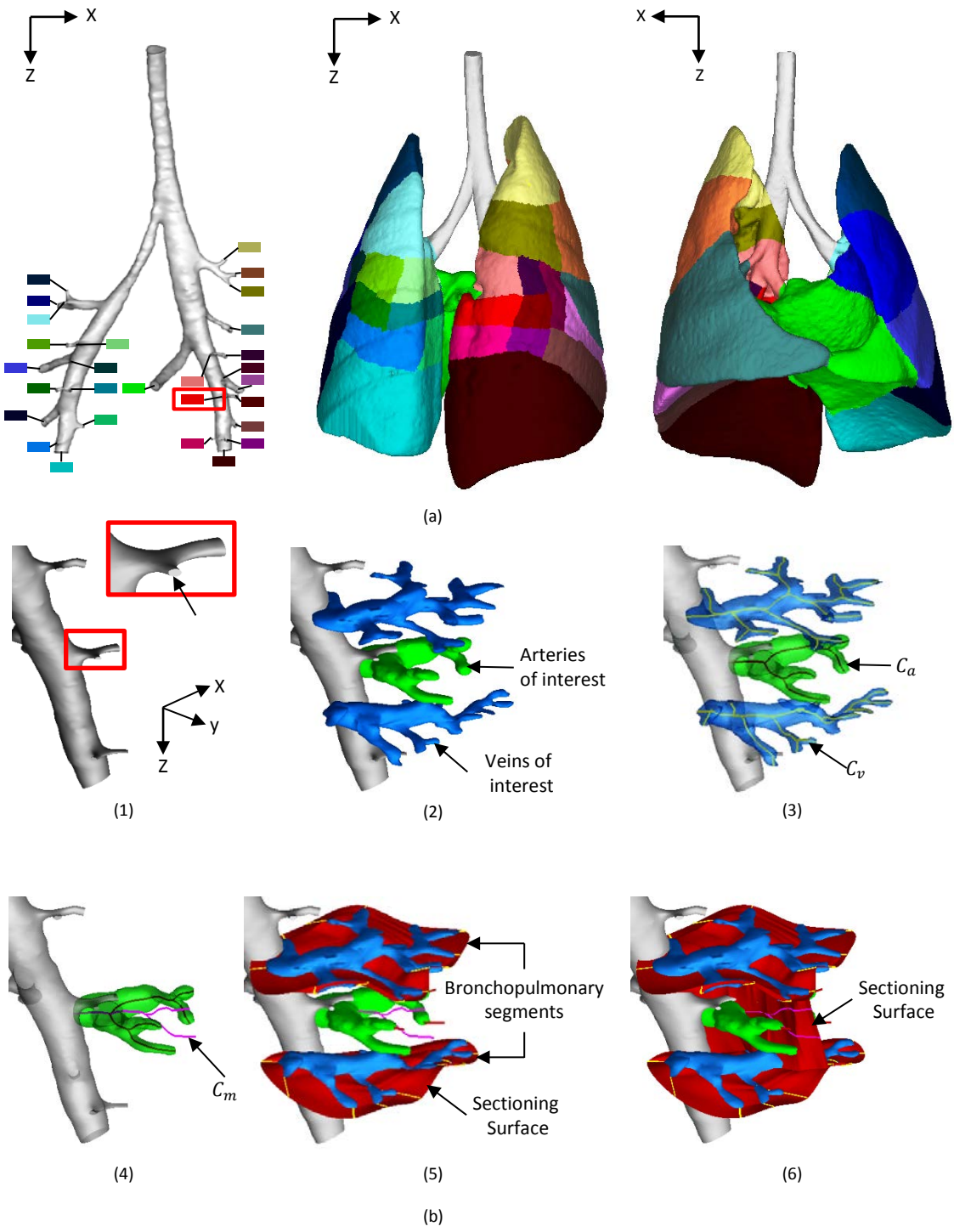

Figure 5: (a) sections of a sample lung volume generated following the proposed technique. Each colour in figure 5 (a) (centre and right) represents the volume of the missing airways associated to each terminal branch in figure 5 (a) (left). (b) the sectioning technique illustrated on a sample terminal branch highlighted by the square inset, (1) the sample terminal branch, (2) the extraction of the blood vessels of interest, (3) generation of the centreline segments C_v and C_a, (4) generation of the midline curve segments C_m, (5) defining the bronchopulmonary segments, (6) defining the lung volume segment.

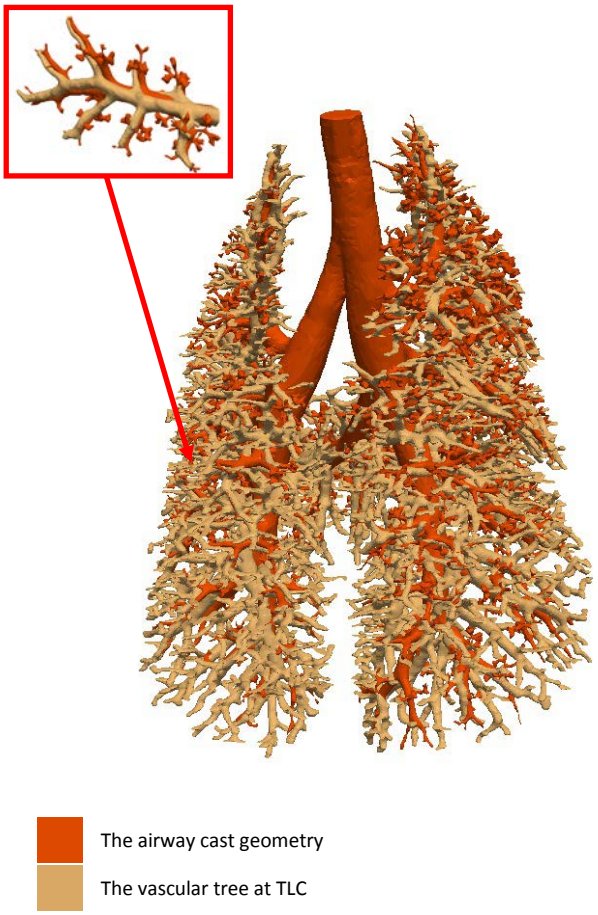

Figure 6: The coupling between the airways cast geometry and the vascular tree geometry following the registration between the airways cast geometry and the airways geometry at TLC. The magnification window illustrates the configuration of a sample airway branch.

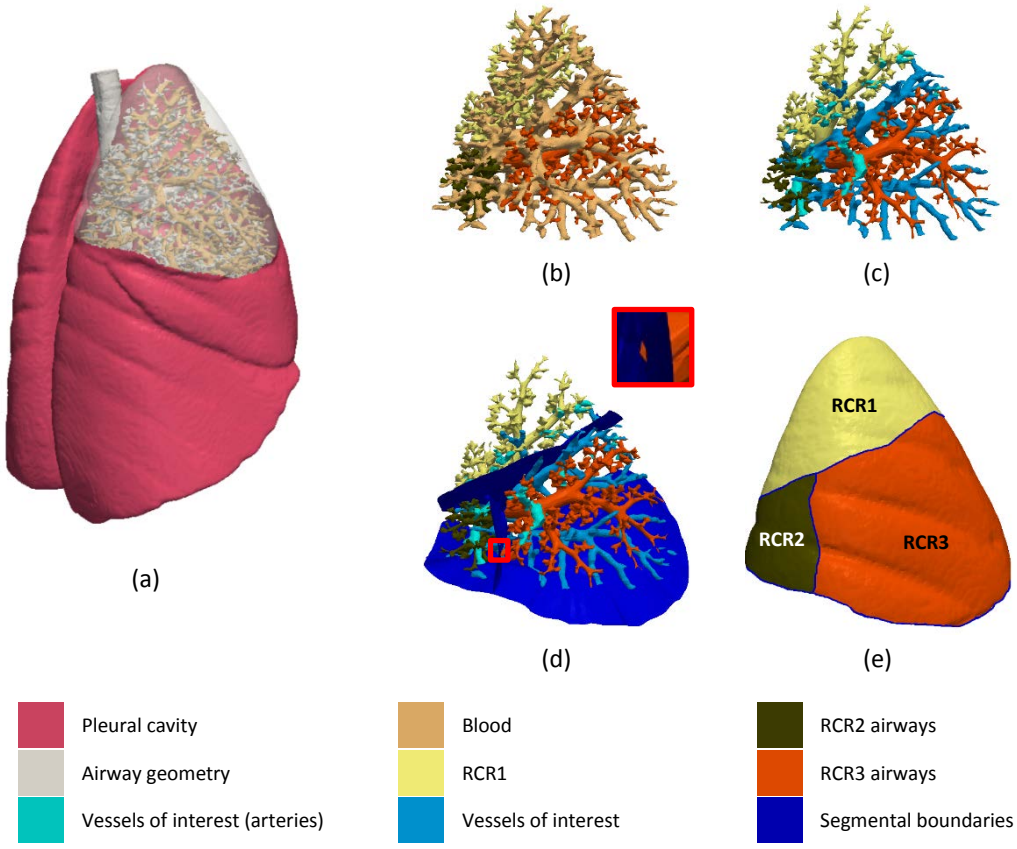

Figure 7: Implementation of the sectioning technique to a cast model of th bronchial airways represented on the right carinal lobe of the Sprauge-Dawley rat. (a) the lobe position in the pleural cavity. (b) the bronchial airways related to each terminal branch of the right carinal lobe coupled to the blood vessel within the lobe. (c) extraction of the vessels of interest. (d) the generation of the boundary surfaces of each segment. (d) the generated segments. The magnification window illustrates a minor geometrical violation observed between the RCR3 segment and the RCR2 segment.

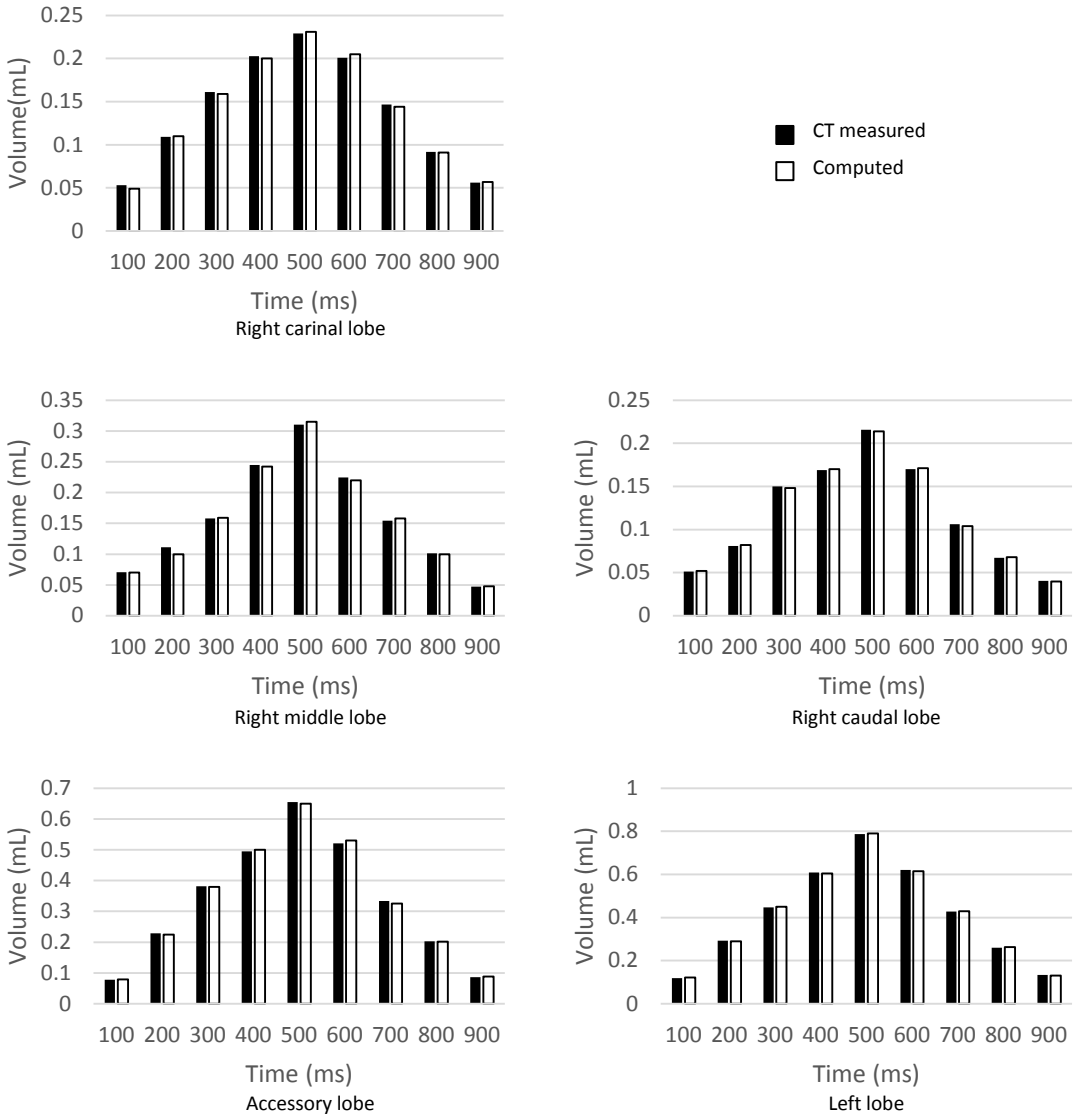

Figure 8: Comparison between the lobar ventilation measured using the proposed sectioning technique to that measured from the dynamic CT data set.